# Identification of density of earth-fill dam using muography

*Toshifumi* Shibata[1#], *Ken* Takahashi[1], *Shin-ichi* Nishimura[1], and *Takayuki* Shuku[1]

[1] *Okayama University, Graduate School of Environmental, Life, Natural Science and Technology, 3-1-1, Tsushima-Naka, Kita-ku, Okayama, 700-8530, Japan.*
[#]*Corresponding author: tshibata@okayama-u.ac.jp*

## ABSTRACT

In recent years, the high probability of large-scale earthquakes occurring in Japan has become a major social concern; and thus, it is urgent that countermeasures and maintenance be implemented for the protection of large-scale societal infrastructures from damage due to these earthquakes. When large-scale societal infrastructures are inspected, an internal diagnosis is required to evaluate the damage condition of the structures in order to see what countermeasures should be planned ahead of the occurrence of any earthquakes. However, conventional methods of diagnosis, such as ground-penetrating radar, have their limitations. Namely, they provide high-precision results in shallow areas, but results with reduced resolution in deeper regions. To overcome the shortcomings associated with these conventional methods of exploring depths out of the investigation range, one approach is to use muography1). This paper investigates the applicability of muon exploration techniques, using cosmic-ray muons, to probe the density of structures inside earth-fill dams.

**Keywords:** muography；earth-fill dam; density.

## 1. Introduction

In the near future, it is anticipated that a large-scale earthquake will occur in Japan, such as a Nankai trough earthquake, making seismic countermeasures for large-scale societal infrastructures extremely crucial. Therefore, an appropriate inspection and internal diagnosis, and repair planning based on them, are particularly necessary. However, conventional methods of diagnosis, such as ground-penetrating radar and electric and seismic prospecting, have their limitations. Namely, ground-penetrating radar has high resolution, but a shallow probing depth, as seen in Fig. 1, while electric and seismic prospecting are susceptible to the effects of vibrations and electrical noises, which are notable drawbacks. Investigations using cosmic ray muons, namely, muography, comprise a method with fewer drawbacks like the probing depth and noise interference.

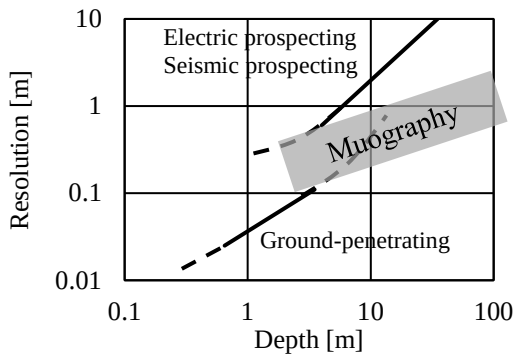


**Figure 1.** Relationship between resolution and depth (modified from Suzuki 2019)

Cosmic ray muons are secondary particles produced by the interaction of interstellar protons with the atmosphere, and nearly a constant amount of them consistently reaches the surface of the earth. The muons have a good penetration ability due to their extremely small size. However, as the density of the material they penetrate or the distance they traverse increases, they lose energy and are more likely to decompose into electrons and neutrinos. Therefore, as the product of the mean density and the vertical distance increases, muons passing through a material lose more energy, resulting in a decrease in the number of muons penetrating the material. The mean density of the material is deduced by the number of detected muons.

In the broader field, muography has been applied to a wide variety of problems. The history of muon research is long and, as early as 1955, attempts were made by George to estimate the density of rock in mines. Alvarez *et al*. (1970) performed muon measurements on a pyramid, and later Morishima *et al*. (2017) discovered a large void in Khufu's Pyramid by muon exploration techniques. In 1979, Malmqvist *et al.* presented theoretical calculations for the mean density of the rock traversed by the muons. Minato (1986) proposed using cosmic ray muons for non-destructive inspections of tall buildings, and Minato (1987) measured the platforms of subway stations in Nagoya City with them. Tanaka *et al*. (2014) investigated the magma dynamics in the Satsuma-Iwojima volcano, while Tanaka *et al*. (2022) expanded the application of muography to atmospheric phenomena and successfully captured tropical cyclones. Yamazaki *et al.* (2022) developed a slim cylindrical muon detector using a plastic scintillator and used it to perform a study on a borehole through the fault zone. Baccani *et al.* (2021) probed the possibility of exploiting the Muon

Transmission Radiography technique for verifying the internal conservation status of levees visibly damaged by animal activities.

This paper investigates the applicability of muon exploration techniques to probe the densities of large-scale structures inside zoned earth-fill dams. The densities of a dam obtained from a muon exploration are compared with those obtained from previous tests to assess its applicability.

## 2. Detector

Muons are obtained by detectors composed of a scintillator and a photomultiplier tube, as seen in Fig. 2. The end part of each detector consists of the scintillator and the photomultiplier tube is incorporated into the cylindrical section connected to it. The transmission of muons through the scintillator is extracted as faint light, converted into electrical signals in the photomultiplier, and then recorded as counts. Two detectors are installed back-to-back into the frame, each with a scintillator diameter of 17.5 cm and spaced at a distance of 100 cm. The arrival direction of the muons can be determined by measuring the muons that have passed through both scintillators. The detectors are connected to a computer via the measurement unit, where the counts of electrical signals are saved as a digital file. Fig. 3 shows the muon measurement system composed of the detectors, measurement unit, and computer. Zenith angle $\theta$ in Fig. 4 is changed by the rotation of the frame of the detectors. Additionally, it is commonly known that muons arrive in a range of directions from close to vertical to nearly horizontal, and that the number of muons reaching the Earth's surface decreases as they approach horizontally.

**Figure 2.** Detectors

The flux, i.e., the muon counts per unit time, unit area, and unit solid angle, that simultaneously pass through two detectors, is measured, and the mean density, multiplied by the vertical distance obtained by Miyake's formula (Miyake, 1973), is determined by Eq. (1).

$$I = \frac{A}{h+H}\left(h\sec\theta + a\right)^{-\alpha} \exp\left(-\beta h \sec\theta\right) \quad (1)$$

where $I$ is the flux, $h$ is the mean density multiplied bythe vertical distance, $\theta$ is the zenith angle, and $A$, $H$, $a$, $\alpha$, and $\beta$ are the parameters with $A$=174 (/cm$^2$/s/sr), $H$=400 (hg/cm$^2$), $a$=11 (hg/cm$^2$), $\alpha$=1.53, and $\beta$=8×10$^{-4}$ (cm$^2$/hg).

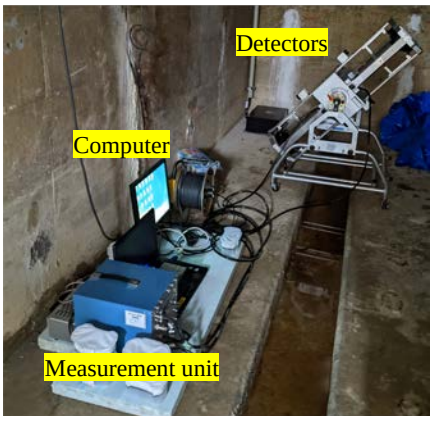


**Figure 3.** Setting of measurement system

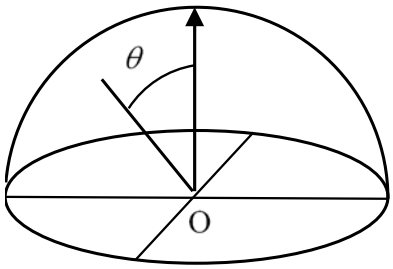


**Figure 4.** Zenith angle

The unit sr represents the unit solid angle. Eq. (1) indicates that the number of muons decreases as zenith angle $\theta$ increases, that is, the detectors approach horizontally. The vertical distance included in parameter $h$ in Eq. (1) is determined from Fig. 4, as will be presented in the next chapter.

The necessary number of muon measurements is herein described. When the number of measured muons is given by a detector, the relationship between the number of muon $N$ and the standard deviation $\sigma$ is represented by Eq. (2).

$$\sigma = \frac{1}{\sqrt{N}} \quad (2)$$

The coefficient of variation $\varepsilon$ (%) to the number $N$ is

$$\varepsilon = \frac{\sqrt{N}}{N} \times 100 \quad (3)$$

Eq. (3) is used to define the error in estimating the density. For example, if only 10 muons are measured, the coefficient of variation will be approximately 30%. When measuring 100 particles, this value becomes 10%; when measuring 1,000 particles, it becomes 3%. If the mean density multiplied by vertical distance $h$ increases, the number of measurements decreases exponentially, resulting in an increase in measurement time. This paper sets the standard required number of muon measurements at 1,000.

## 3. Outline of earth-fill dam

Fig. 5 presents a cross-sectional view of the target earth-fill dam with a height of 49.7 m, crest length of 250 m, embankment volume of 535,000 m$^3$, total storage

capacity of 1,308,000 $m^3$, effective storage capacity of 1,186,000 $m^3$, drainage area of 8.1 $km^2$, and reservoir area of 10 ha. The earth-fill dam is composed of five zones, namely, impervious zones #1 and #2, a filter zone, and pervious zones #1 and #2. The inspection gallery is located at the foot of the dam under impervious zone #1. In Fig. 5, the seven angles, namely, 0°, 10°, 20°, 30°, 40°, 50°, and 60° represent the zenith angles of the muon detectors.

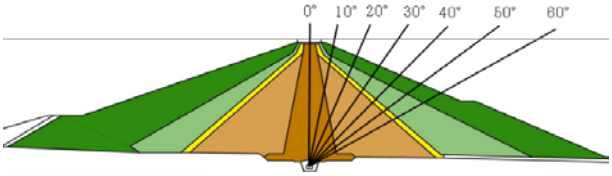


**Figure 5.** Cross-sectional view of earth-fill dam

**Table 1.** Density of each zone

| | Zone | Type | Material | Density ($g/cm^3$) |
|---|---|---|---|---|
| | #1 | Impervious zone | Decomposed granite | 2.07 |
| | #2 | Impervious zone | Decomposed granite | 2.08 |
| | #3 | Filter zone | Graded crushed stone | 1.97 |
| | #4 | Pervious zone | Weathered granite | 2.11 |
| | #5 | Pervious zone | Granite | 2.14 |

Table 1 summarizes the density of each zone obtained by density tests previously conducted, and the density is conventionally called the "pre-test density". The colors in the first column correspond to the zone colors in Fig. 5. The muon measurement system is installed in the inspection gallery, while the zenith angle of the detectors is varied at intervals of 10°.

## 4. Results

Table 2 shows the relationship between the densities computed from the number of measured muons and the zenith angles. The computed density is conventionally called the "identified density". When more muons are being measured, the measurement time becomes longer. Although the measurement count of the muons at the zenith angle of 20° is less than 1,000, the coefficient of variation $\varepsilon$ in Eq. (3) is 3.34%. Since there is little difference in the coefficient of variation, compared to when there is a count of 1,000, the result at the zenith angle of 20° is used. The measured muons in the zenith angle of 0° are passing through only impervious zone #1, while the muons in the other angles are penetrating through multiple zones. The identified density of 2.045 in zone #1 in Table 2 matches the pre-test density of 2.07 in Table 1 well, because the muons in the zenith angle of 0° only penetrate zone #1.

Subsequently, the density of each zone is determined. Eq. (4) represents the mean density multiplied by the vertical distance at each zenith angle.

**Table 2.** Results of measurement of muons and densities

| Zenith angle | Measurement count of muons | Measurement time (hour) | Density ($g/cm^3$) |
|---|---|---|---|
| 0° | 2386 | 504 | 2.045 |
| 10° | 4338 | 888 | 2.033 |
| 20° | 894 | 167 | 2.004 |
| 30° | 1978 | 383 | 2.073 |
| 40° | 1628 | 337 | 2.119 |
| 50° | 1239 | 288 | 2.175 |
| 60° | 1151 | 336 | 2.316 |

$$\rho_{mi} l_{mi} = \sum_{j=1}^{5} \rho_j l_{ij} \tag{4}$$

where $\rho_{mi}$ is the identified density in Table 2 at the $i$-th zenith angle, $l_{mi}$ indicates the vertical distance at the $i$-th zenith angle, where $i$=0, 1, 2, 3, 4, 5 represents the zenith angles of 0°, 10°, 20°, 30°, 40°, and 50°, $\rho_j$ is the density in the $j$-th zone, and $l_{ij}$ is the vertical distance at the $i$-th zenith angle and the $j$-th zone. For example, the 1st zone, namely $j$=1, is impervious zone #1. $\rho_{mi}\, l_{mi}$ in Eq. (4) is equal to $h$ corresponding to the zenith angle. The least squares method is adopted to identify the five densities in the $j$-th zone using the identified densities at each zenith angle in Table 2, while vertical distances $l_{ij}$ and $l_{mi}$ are determined from Fig. 5.

Table 3 presents a comparison between the identified densities from the number of measured muons and the pre-test densities. Although the identified density in zone #1 is close to the pre-test density, there is a difference between them in the other zones. The results suggest that the slight error occurring during the muon measurements affects the identified density, since the pre-test density of each zone is almost the same.

**Table 3.** Comparison between identified densities and pre-test densities in five zones

| Zone | Identified density ($g/cm^3$) | Pre-test density ($g/cm^3$) |
|---|---|---|
| #1 | 2.363 | 2.07 |
| #2 | 0.925 | 2.08 |
| #3 | -2.072 | 1.97 |
| #4 | 5.043 | 2.11 |
| #5 | 3.479 | 2.14 |

Next, the five zones are grouped into two main zones, namely, the impervious zone and the pervious zone. The impervious zone consists of zones #1, #2, and filter zone #3, while the pervious zone consists of zones #4 and #5. Table 4 compares the identified densities divided into the two zones with the mean pre-test densities of the two zones, where the pre-test densities are the mean values. The identified density of the impervious zone is slightly

smaller than the pre-test density, whereas the identified density of the pervious zone is slightly larger. When divided into two zones, it is closer to the pre-test density compared to when it is divided into five zones.

This study investigates only the density on the downstream side of the dam using muography. If muon measurements are carried out on the upstream side of the dam, it seems that it would be possible to estimate the water level of the dam using the results of the density on the downstream side of the dam.

Although the difficulty of identifying the density of each zone is shown, the applicability of muon exploration techniques to earth-fill dams is presented in this paper.

**Table 4.** Comparison between identified densities and pre-test densities in two zones

| | Identified density ($g/cm^3$) | Pre-test density ($g/cm^3$) |
|---|---|---|
| Impervious zone | 1.790 | 2.075 |
| Pervious zone | 2.933 | 2.073 |

## 5. Conclusions

This paper presented the applicability of muon exploration techniques for probing the densities of structures inside earth-fill dams. Muon measurements were performed while changing the zenith angle of the detectors, and the densities were identified by the number of measured muons. The identified density in zone #1 was found to be very close to the pre-test density, because the muons in the zenith angle of 0° only pass through zone #1.

It seems that by applying the density obtained from muon measurements taken downstream, along with the density obtained from muon measurements taken upstream, it would be possible to estimate the water level of the dam.

Although the difficulty of identifying the density of each zone was exhibited, this study confirmed the applicability of muon exploration techniques to earth-fill dams.

## Acknowledgements

The valuable suggestions and comments by Dr. Keiichi Suzuki of Kawasaki Geological Engineering Co., Ltd. are gratefully acknowledged.

## References

Alvarez, L. W., Anderson, J. A., EI Bedwei, F., Burkhard, J., Fakhry, A., Girgis, A., Goneid, A., Hassan, F., Iverson, D., Lynch, G., Miligy, Z., Moussa, A. H., Sharkawi, M., and Yazolino, L. 1970. “Search for Hidden Chambers in the Pyramids.”, *Science*, 167, 832-839. https://www.science.org/doi/10.1126/science.167.3919.832

Baccani, G., Bonechi, L., Bongi, M., Casagli, N., Ciaranfi, R., Ciulli, V., D'Alessandro, R., Gonzi, S., Lombardi, L., Morelli, S., Nocentini, M., Pazzi, V., Tacconi S., and C., Viliani, L. 2021. “The reliability of muography applied in the detection of the animal burrows within River Levees validated by means of geophysical techniques.” *Journal of Applied Geophysics*, 191, https://doi.org/10.1016/j.jappgeo.2021.104376

George, E. P. 1955. “Cosmic rays measure overburden of tunnel.” *Commonwealth Engineer*, 42(12), 455-457.

Malmqvist, L., Jinsson, G., Kristiansson, K., and Jacobsson, L. 1979. “Theoretical studies of in-situ rock density determinations using underground cosmic-ray muon intensity measurements with application in mining geophysics.” *Geophysics*, 44(9), 1549-1569. https://doi.org/10.1190/1.1441026

Minato, S. 1986. “Bulk Density Estimates of Buildings using Cosmic Rays.” *Applied Radiation and Isotopes*, 37, 941-946.

Minato, S. 1987. “Feasibility study on cosmic-ray non-destructive testing through structural analysis of subway stations.” *NDT International*, 20, 231-234.

Miyake, S. 1973. “Rapporteur paper on muons and neutrinos.” *13th International Cosmic Ray Conference*, 5, 3638–3655.

Morishima, K., Kuno, M., Nishio, A., Kitagawa, N. Namabe, Y., Moto, M., Takasaki, F., Fujii, H., Satoh, K., Kodama, H., Hayashi, K., Odaka, S., Procureur, S., Attié, D., Bouteille, S., Clavet, D., Filosa, C., Magnier, P., Mandjavidze, I., Riallot, M., Marini, B., Gable, P., Date, Y., Sugiura, M., Elshayeb, Y., Elnady, T., Ezzy, M., Guerriero, E., Steiger, V., Serikoff, N., Mouret, J. B., Cjarlés, B., Helal, H., and Tayoubi, M. 2017. “Discovery of a big void in Khufu’s Pyramid by Observation of Cosmic-ray Muons.” *Nature*, 552, 386-390, 10.1038/nature24647. https://www.nature.com/articles/nature24647

Suzuki, K. and Kanazawa, S. 2016. “Exploration Technology Using Cosmic Ray Muons for Engineering Geology.” *Journal of the Japan Society of Engineering Geology*, 57(6), 266-276 (in Japanese). https://doi.org/10.5110/jjseg.57.266

Suzuki, K. 2019. “Exploration of cavities by cosmic ray muons.” (in Japanese) https://www.chubu-geo.org/publish/No67/no067.html

Tanaka, H. K. M., Kasugaya, T., and Shinohara, H. 2014. “Radiographic visualization of magma dynamics in an erupting volcano.” *Nature communications*, 10.1038/ncomms4381. https://www.nature.com/articles/ncomms4381

Tanaka, H. K. M., Gluyas, J., Holma, M., Joutsenvaara, J., Kuusiniemi, P., Leone, G., Presti, D. L., Matsushima, J., Oláh, L., Steigerwald, S., Thompson, L. F., Usoskin, I., Poluianov, S., Varga, D., and Yokota, Y. 2022. “Atmospheric Muography for Imaging and Monitoring Tropic Cyclones.” *Scientific Reports*, 12. https://www.nature.com/articles/s41598-022-20039-4

Yamazaki, K., Taketa, A., Ikeda, D., and Omura, K. 2022. “Development of detector and method for density structure measurement of fault zones using cosmic ray muons.” *Nuclear Instruments and Methods in Physics Research Section A: Accelerators, Spectrometers, Detectors and Associated Equipment*, 1031, https://doi.org/10.1016/j.nima.2022.166518